AIAA 98-3295

Aeroelastic Calculations Based on Three-Dimensional Euler Analysis

Milind A. Bakhle, Rakesh Srivastava, and Theo G. Keith, Jr.
University of Toledo
Toledo, Ohio 43606

George L. Stefko
NASA Lewis Research Center
Cleveland, Ohio 44135

34th AIAA/ASME/SAE/ASEE
Joint Propulsion Conference & Exhibit
July 13-15, 1998 / Cleveland, OH

AIAA-98-3295

AEROELASTIC CALCULATIONS BASED ON THREE-DIMENSIONAL EULER ANALYSIS

Milind A. Bakhle,* Rakesh Srivastava,* and Theo G. Keith, Jr.**
University of Toledo, Toledo, Ohio 43606

George L. Stefko ***
NASA Lewis Research Center
Cleveland, Ohio 44135

Abstract

This paper presents representative results from an aeroelastic code (TURBO-AE) based on an Euler / Navier-Stokes unsteady aerodynamic code (TURBO). Unsteady pressure, lift, and moment distributions are presented for a helical fan test configuration which is used to verify the code by comparison to two-dimensional linear potential (flat plate) theory. The results are for pitching and plunging motions over a range of phase angles. Good agreement with linear theory is seen for all phase angles except those near acoustic resonances. The agreement is better for pitching motions than for plunging motions. The reason for this difference is not understood at present. Numerical checks have been performed to ensure that solutions are independent of time step, converged to periodicity, and linearly dependent on amplitude of blade motion. The paper concludes with an evaluation of the current state of development of the TURBO-AE code and presents some plans for further development and validation of the TURBO-AE code.

Introduction

There is an ongoing effort to develop technologies to increase the fuel efficiency of commercial aircraft engines, improve the safety of engine operation, reduce the emissions, and reduce engine noise. With the development of new designs of ducted fans, compressors, and turbines to achieve these goals, a basic aeroelastic requirement is that there should be no flutter or high resonant blade stresses in the operating regime. In order to verify the aeroelastic soundness of the design, an accurate prediction of the unsteady aerodynamics and structural dynamics of the propulsion component is required. The complex geometry, the presence of shock waves and flow separation makes the modeling of the unsteady aerodynamics a difficult task. The advanced blade geometry, new blade materials and new blade attachment concepts make the modeling of the structural dynamics a difficult problem.

Computational aeroelastic modeling of fans, compressors, and turbines requires many simplifying assumptions. For instance, flutter calculations are typically carried out assuming that the blade row is isolated. This simplifies the structural dynamics formulation and the unsteady aerodynamic calculations considerably.

For an isolated blade row flutter calculation, the modeling of the unsteady aerodynamics is the biggest challenge. Many simplifying assumptions are made

* Senior Research Associate
** Distinguished University Professor
*** Branch Manager, Machine Dynamics Branch

in the modeling of the unsteady aerodynamics. In the past, panel methods based on linear compressible small-disturbance potential theory have been used to model the unsteady aerodynamics and aeroelasticity of fans in subsonic flow; see for example [1,2]. The major limitations of this type of analysis are the neglect of transonic, vortical, and viscous flow effects in the model. These inherent limitations in the model preclude its use in a majority of practical applications. A full potential unsteady aerodynamic analysis has been used with a modal structural dynamics method to model the aeroelastic behavior of fan blades [3,4]. Although the full potential aerodynamic formulation is able to model transonic effects (limited to weak shocks), the vortical and viscous effects are still neglected. For example, the blade tip vortex, or a leading-edge vortex is not modeled. Recently, researchers [5-10] have also developed inviscid and viscous unsteady aerodynamic analyses for vibrating blades.

For aeroelastic problems in which viscous effects play an important role (such as flutter with flow separation, or stall flutter, and flutter in the presence of shock and boundary-layer interaction), a more advanced aeroelastic computational capability is required. The authors of this paper have earlier presented [11] some results from the TURBO-AE aeroelastic code. Initial calculations were restricted to in-phase (zero phase angle) blade motions and inviscid flow. In a later paper [12], results were presented for zero and non-zero phase angle motions and viscous flow. In these calculations, multiple blade passages were modeled for non-zero phase angle motions. Most recently [13], results have been presented using a single blade passage with phase-lag periodic boundary conditions to model arbitrary phase angle motions.

This paper presents unsteady pressure, lift, and moment distributions due to blade vibration over a range of phase angles for verification of the TURBO-AE aeroelastic code. For non-zero phase angle motions, phase-lag periodic boundary conditions are used. The configuration selected is a helical fan. The geometry and flow conditions are chosen to minimize non-linear and three-dimensional effects since the intent is to verify the code by comparison with two-dimensional linear potential (flat plate) theory.

Aeroelastic Code – TURBO-AE

This section briefly describes the aeroelastic code (TURBO-AE); previous publications [11-13] provide additional details. The TURBO-AE code is based on an unsteady aerodynamic Euler / Navier-Stokes code (TURBO), developed separately [14,15]. The TURBO code provides all the unsteady aerodynamics to the TURBO-AE code.

The TURBO code was originally developed [14] as an inviscid flow solver for modeling the flow through turbomachinery blade rows. Additional developments were made [15] to incorporate viscous effects into the model. This Reynolds-averaged Navier Stokes unsteady aerodynamic code is based on a finite volume scheme. Flux vector splitting is used to evaluate the flux Jacobians on the left hand side of the governing equations [14] and Roe's flux difference splitting is used to form a higher-order TVD (Total Variation Diminishing) scheme to evaluate the fluxes on the right hand side. Newton sub-iterations are used at each time step to maintain higher accuracy. Symmetric Gauss-Seidel iterations are applied to the discretized equations. A Baldwin-Lomax algebraic turbulence model is used in the code.

The TURBO-AE code assumes a normal mode representation of the structural dynamics of the blade. A work-per-cycle method is used to determine aeroelastic stability (flutter). Using this method, the motion of the blade is prescribed to be a harmonic vibration in a specified in-vacuum normal mode with a specified frequency (typically the natural frequency). The work done on the vibrating blade by aerodynamic forces during a cycle of vibration is calculated. If work is being done *on* the blade by the aerodynamic forces at the end of a vibration cycle, the blade is dynamically unstable, since it will result in extraction of energy from the flow, leading to an increase in amplitude of oscillation of the blade.

The inlet/exit boundary conditions used in this code are described in [16-18]. For cases in which the blade motions are not in-phase, phase-lag periodic boundary conditions based on the direct store method are used.

Results

In this section, results are presented which serve to verify the TURBO-AE code. The test configuration selected is a helical fan [16]. This configuration consists of a rotor with twisted flat plate blades enclosed in a cylindrical duct with no tip gap. This configuration was developed by researchers [16] to provide a relatively simple test case for comparison

with two-dimensional analyses. The geometry is such that three-dimensionality of the flow is minimized.

The parameters of this three-dimensional configuration are such that the mid-span location corresponds to a flat plate cascade with a stagger angle of 45 deg. and unit gap-to-chord ratio operating in a uniform mean flow at a Mach number of 0.7 parallel to the blades. The rotor has 24 blades with a hub/tip ratio of 0.8. The inlet flow (axial) Mach number used in this calculation is 0.495, which results in a relative Mach number of approximately 0.7 at the mid-span section. The results presented are for inviscid runs of the TURBO-AE code.

The grid used for the calculations is 141×11×41 in one blade passage. On each blade surface, 81 points are located in the chordwise direction and 11 points in the spanwise direction. The inlet and exit boundaries are located at an axial distance of approximately 0.7 chord lengths from the blade leading and trailing edges. To begin, a steady solution is obtained for this configuration. The steady flowfield consists of uniform flow at each radial location.

Aeroelastic calculations are performed starting from the steady solution. Calculations have been performed for harmonic blade vibration in plunging and pitching modes, separately. The pitching is about the mid-chord. The prescribed mode shapes are such that the amplitude of vibration does not vary along the span. This choice of mode shapes is meant to reduces the three-dimensionality of the unsteady flowfield for ease of comparison with two-dimensional analyses.

The vibration frequency is selected so that the non-dimensional reduced frequency based on blade chord is 1.0 at the mid-span. A study was performed to determine the sensitivity of numerical results to the number of time steps used in each cycle of blade vibration. Calculations were done with 100, 200, and 300 time steps per cycle of vibration for 0 deg. phase angle plunging motion. The time step was varied so as to keep the vibration time period (or frequency) fixed. Figure 1 shows the work-per-cycle from this study. As the flowfield reaches periodicity, it can be seen that the results are nearly identical for 200 and 300 time steps per cycle. These results differ slightly from the results for 100 time steps per cycle. Figure 2 shows the unsteady pressure difference for the same three numbers of time steps per cycle. The results for 200 and 300 time steps per cycle are indistinguishable. Based on such calculations, it was determined that 200 time steps per cycle provided adequate temporal resolution for the selected vibration frequency. All results presented here have been obtained using 200 time steps per cycle.

The non-dimensional time step used in the calculations (with 200 time steps per cycle) is 0.045, which results in a maximum CFL number of 60.5. The amplitude of blade vibrations in the calculation is a pitching amplitude of 0.2 deg. or a plunging amplitude of 0.1% chord. In all cases, calculations were continued for a number of cycles of blade vibration to allow the flowfield to become periodic. Initial calculations with phase angles of 0, 45, 90, 135, 180, 225, 270, and 315 deg. were continued for 15 cycles of blade vibration to ensure periodicity. Later calculations with intermediate phase angles (22.5, 67.5, ... , and 337.5 deg.) were continued only for 10 cycles of blade vibration due to insufficient computational resources. In an earlier study [13], it was shown that, for the various phase angles studied, the flowfield became periodic after about 7-10 cycles of blade vibration. Hence, the 10 or 15 cycles used in the present work were considered adequate to reach periodicity.

Figure 3 shows the unsteady moment about mid-chord (in complex form) for pitching blade motion about the mid-chord. These results are from the mid-span location and were calculated using the first harmonic of the unsteady blade surface pressure difference. Semi-analytical results from two-dimensional linear potential (flat plate) theory [19] are included for comparison.

The overall level of agreement between TURBO-AE results and linear theory is very good, with exceptions to be discussed in the following paragraph. For subsonic flows and small amplitude of blade motions, it is expected that there will be no significant difference between the Euler and linear potential results. Hence, the observed agreement is not surprising and provides a basic verification of the TURBO-AE code. It may be noted that the parameters of the present configuration were selected [16] to allow exactly this type of a verification by comparison to two-dimensional analyses.

In Figure 3, some deviation from linear theory is seen in the results for phase angles of 112.5 and 135 deg., and to a lesser extent for phase angles of 157.5 and 315 deg. All these phase angles fall near conditions of

acoustic resonance (or cut-off conditions) in the corresponding two-dimensional flat plate cascade. The acoustic resonances occur at phase angles of 107.3 and 330.6 deg.; these values are marked on the phase angle axis of Figure 3 for reference. The phase angles between these resonances are associated with sub-resonant [20] (cut-off) conditions in which all disturbances attenuate away from the cascade. No disturbances propagate in the upstream or downstream directions under sub-resonant conditions. The phase angles between 0 and 107.3 deg. and between 330.6 and 360 deg. are associated with super-resonant (cut-on) conditions in which at least one disturbance propagates in either the far upstream or downstream direction.

The significance of the sub-resonant and super-resonant conditions to computational aeroelasticity can be explained as follows. Since the typical computational domain does not extend very far from the blade row or cascade, the inlet/exit boundary conditions must minimize (or eliminate) the reflection of disturbances generated by the vibration of the blades. For sub-resonant conditions, it may be possible to reduce the reflected disturbances by moving the boundary farther away from the blade row. This is not possible for super-resonant conditions. From Figure 3, it can be seen that the results from TURBO-AE agree well with linear theory for both sub-resonant and super-resonant conditions. It may be also recalled that the computational inlet/exit boundaries are located quite near (0.7 axial chord lengths from leading/trailing edges) the blade row in the present calculations.

Figure 4 shows the unsteady lift (in complex form) for plunging blade motion. As noted for the pitching results, these results are also from the mid-span location and were also calculated using the first harmonic of the unsteady blade surface pressure difference. Results from linear potential theory are included in Figure 4 for comparison. The overall level of agreement with linear theory is good, but not as good as that for pitching motion (Figure 3). The source of such a difference between the plunging and pitching results is not understood. However, such differences in agreement have been noted by other researchers [16,17] for a different configuration. In addition, deviations are observed close to the acoustic resonances, as for pitching.

Figure 5 shows the unsteady blade surface pressure difference (first harmonic) at the mid-span location for pitching blade motion about the mid-chord. Results are presented for phase angles values between 0 and 360 deg. in steps of 22.5 deg. In each case, the linear theory results are included for comparison. In most cases, the agreement with linear theory is very good. The exceptions occur at phase angles near acoustic resonance conditions, as noted earlier in the description of the unsteady moment (Figure 3). It is worth noting that, in this case, the integrated results in Figure 3 accurately represent the level of agreement with linear theory, without obscuring any differences in the details of the pressure distributions.

Figure 6 shows the unsteady blade surface pressure difference (in complex form) for plunging blade motion. The level of agreement with linear theory is not as good as for pitching, as reflected in the unsteady lift (Figure 4). The most serious deviations from linear theory are restricted to the phase angles near conditions of acoustic resonance.

Some of the results for plunging motion (Figure 6) show an irregular (unsmooth) variation in the unsteady pressure distribution which is not seen in any of the results for pitching motion (Figure 5). This uneven variation can be seen in the plunging results in Figures 6b, 6d, 6f, 6h, 6j, 6l, 6n, and 6p for phase angles of 22.5, 67.5, 112.5, ... , and 337.5 deg. One common characteristic of these results is that these were all generated on a workstation and may therefore suffer from some precision-related numerical problem. However, it is surprising to note that the corresponding results for pitching motion (also computed on a workstation) are quite smooth and do not show such unevenness. A re-calculation of selected plunging results on a super-computer does indeed eliminate the unevenness in pressure variation, but the pressure distributions remain substantially unchanged from those presented in Figure 6.

Note that all the TURBO-AE results presented are the first harmonic components of the unsteady variations. The higher harmonics are extremely small for these calculations, indicating the linearity of the unsteady flow. Previous results [12] had shown a nonlinear dependence on amplitude for certain cases for pitching amplitudes of blade vibration of 2 deg., but not at the 0.2 deg. amplitude used in the present calculations.

To investigate the effect of some numerical parameters on the results for phase angle of 112.5 deg. (where the maximum deviation from linear

theory is observed), the following calculations were done. The number of time steps per cycle was doubled from 200 to 400, with a corresponding halving of the time step. The unsteady pressure results showed no changes within plotting accuracy, indicating adequate temporal resolution. Similarly, the number of cycles of oscillation was doubled from 10 to 20 to examine possible lack of periodicity. No change in the unsteady pressure results was observed within plotting accuracy. The deviations in the regions of acoustic resonances may possibly be reduced by the use of finer grids. But, such a grid refinement study has not yet been performed.

Concluding Remarks

An aeroelastic analysis code named TURBO-AE has been developed and is being verified and validated. The starting point for the development was an Euler / Navier-Stokes unsteady aerodynamic code named TURBO. Some verification has been done by running the code for a helical fan test configuration. Results have been presented for pitching and plunging blade motions over a range of phase angles. The results compare well with results from a linear potential analysis. This agreement is expected for subsonic flows for which the calculations were made and for the relatively small amplitudes of blade motion.

The agreement is not as good for plunging motion as for pitching motion. The reason for this difference is not understood at present. Also, deviations are observed for values of phase angles near acoustic resonance conditions. The solutions are shown to be independent of the time step, converged to periodicity, and linearly dependent on amplitude of blade motion. This test case provides a basic verification of the TURBO-AE code. It also shows the need to perform a grid refinement study as a possible way to resolve the deviations from linear theory near acoustic resonance conditions and for plunging motion. For plunging motion, some results are affected by precision-related numerical problems, as seen from uneven pressure distributions. But, the elimination of these precision problems does not change the pressure distributions substantially, apart from making the variations smooth.

It is necessary to further verify the TURBO-AE using different standard test configurations to compare with experimental data and other code predictions. This is being done in collaboration with other researchers. Also, it is necessary that the TURBO-AE code be exercised to evaluate its ability to analyze and predict flutter for conditions in which viscous effects are significant. This work is also currently in progress.

Acknowledgments

The authors would like to gratefully acknowledge the support of Project Managers Peter G. Batterton (Subsonic Systems Office) and John E. Rohde (Advanced Subsonic Technology Project Office) at NASA Lewis Research Center. Computational resources for this research were provided by NAS.

References

[1] Williams, M. H., "An Unsteady Lifting Surface Method for Single Rotation Propellers", NASA CR-4302, 1990.

[2] Kaza, K. R. V. et al., "Analytical Flutter Investigation of a Composite Propfan Model", Journal of Aircraft, Vol. 26, No. 8, pp. 772-780, 1989.

[3] Bakhle, M. A., and Reddy, T. S. R., "Unsteady Aerodynamics and Flutter of Propfans Using a Three-Dimensional Full-Potential Solver", AIAA Paper 93-1633, 1993.

[4] Bakhle, M. A. et al., "Unsteady Aerodynamics and Flutter Based on the Potential Equation", AIAA Paper 93-2086, 1993.

[5] Srivastava, R. and Reddy, T. S. R., "Aeroelastic Analysis of Ducted Rotors", presented at the 1995 International Mechanical Engineering Congress and Exposition, 1995.

[6] Hall, K. C., "Calculation of Three-Dimensional Unsteady Flows in Turbomachinery Using the Linearized Harmonic Euler Equations", AIAA Paper 92-0665, 1992.

[7] He, L., and Denton, J. D., "Three-Dimensional Time-Marching Inviscid and Viscous Solutions for Unsteady Flows Around Vibrating Blades", ASME Paper 93-GT-92, 1993

[8] Gerolymos, G. A., and Vallet, I., "Validation of 3D Euler Methods for Vibrating Cascade Aerodynamics", ASME Paper 94-GT-294, 1994.

[9] Peitsch, D., et al., "Prediction of Unsteady 2D Flow in Turbomachinery Bladings", Proceedings of

the 7th International Symposium on Unsteady Aerodynamics and Aeroelasticity of Turbomachines, Fukuoka, Japan, September 25-29, 1994

[10] Carstens, V., "Computation of Unsteady Transonic 3D-Flow in Oscillating Turbomachinery Bladings by an Euler Algorithm with Deforming Grids", Proceedings of the 7th International Symposium on Unsteady Aerodynamics and Aeroelasticity of Turbomachines, Fukuoka, Japan, September 25-29, 1994.

[11] Bakhle, M. A. et al., "Development of an Aeroelastic Code Based on an Euler / Navier-Stokes Aerodynamic Solver", ASME Paper 96-GT-311, 1996.

[12] Bakhle, M. A. et al., "A 3D Euler / Navier-Stokes Aeroelastic Code for Propulsion Applications", AIAA Paper 97-2749, 1997.

[13] Srivastava, R. et al., "Application of Time-Shifted Boundary Conditions to a 3D Euler / Navier-Stokes Aeroelastic Code", ASME Paper 98-GT-42, 1998.

[14] Janus, J. M., "Advanced 3-D CFD Algorithm for Turbomachinery", Ph.D. Dissertation, Mississippi State University, Mississippi, 1989.

[15] Chen, J. P., "Unsteady Three-Dimensional Thin-Layer Navier-Stokes Solutions for Turbomachinery in Transonic Flow", Ph.D. Dissertation, Mississippi State University, Mississippi, 1991.

[16] Montgomery, M. D., and Verdon, J. M., "A Three-Dimensional Linearized Unsteady Euler Analysis for Turbomachinery Blade Rows", NASA Contractor Report 4770, 1997.

[17] Chuang, H. A., and Verdon, J. M., "A Nonlinear Numerical Simulator for Three-Dimensional Flows Through Vibrating Blade Rows", ASME Paper 98-GT-018, 1998.

[18] Chuang, H. A., and Verdon, J. M., "A Numerical Simulator for Three-Dimensional Flows Through Vibrating Blade Rows", NASA Contractor Report to be published, 1998.

[19] Smith, S. N., "Discrete Frequency Sound Generation in Axial Flow Turbomachines", R&M 3709, British Aeronautical Research Council, London, England, UK, 1972.

[20] Verdon, J. M., "The Unsteady Flow in the Far Field of an Isolated Blade Row", Journal of Fluids and Structures, Vol. 3, No. 2, pp. 123-149, 1989.

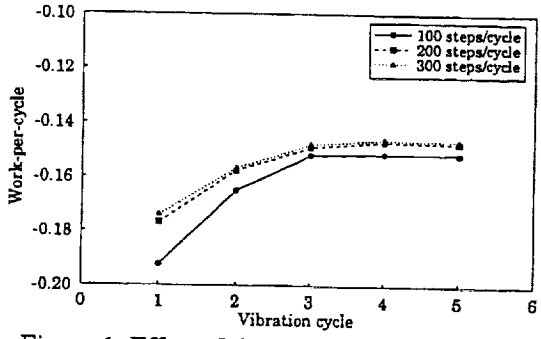

Figure 1: Effect of time steps per cycle on work.

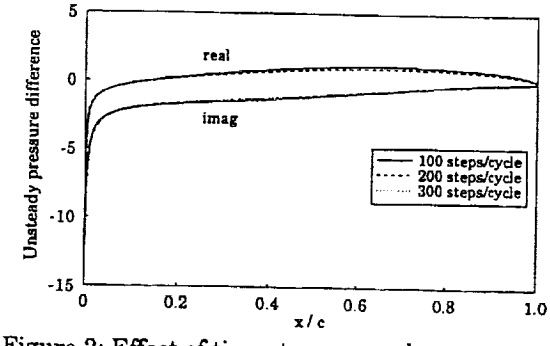

Figure 2: Effect of time steps per cycle on pressure.

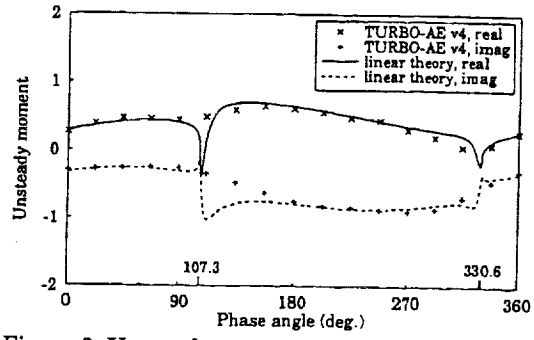

Figure 3: Unsteady moment for pitching motion.

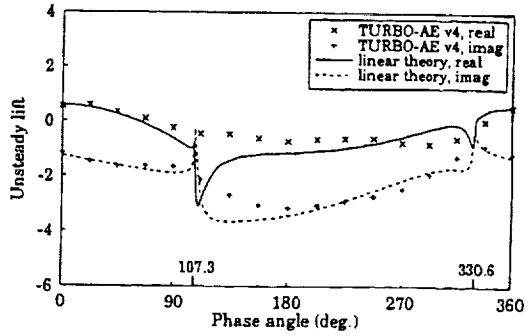

Figure 4: Unsteady lift for plunging motion.

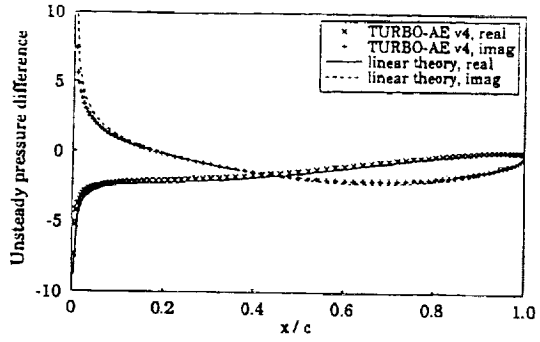

(a) 0 deg. pitching

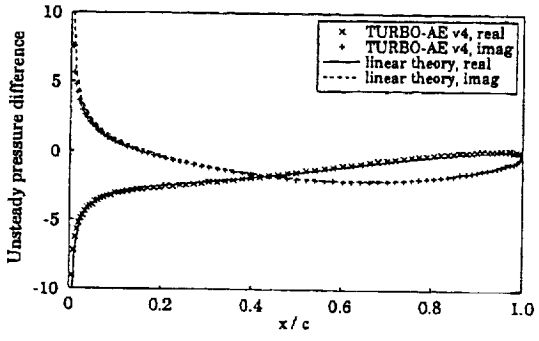

(b) 22.5 deg. pitching

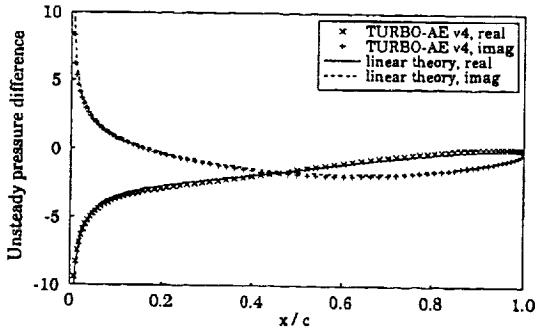

(c) 45 deg. pitching

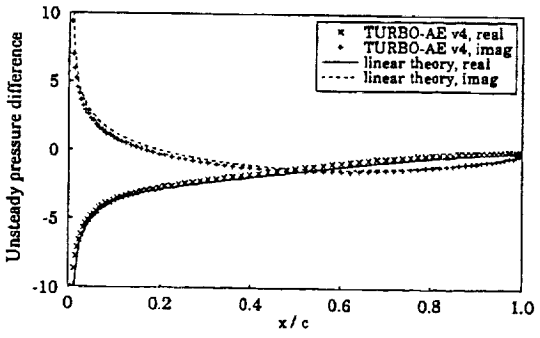

(d) 67.5 deg. pitching

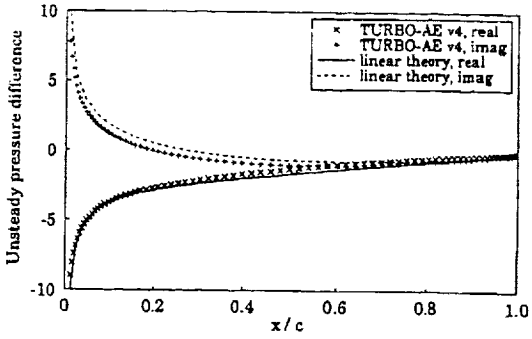

(e) 90 deg. pitching

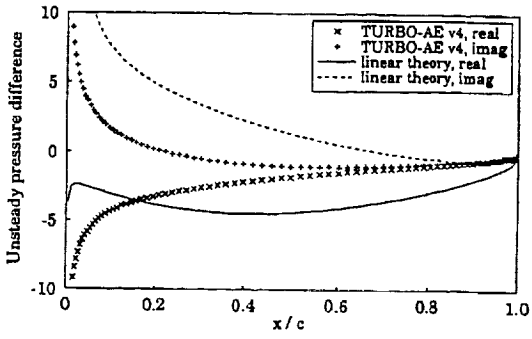

(f) 112.5 deg. pitching

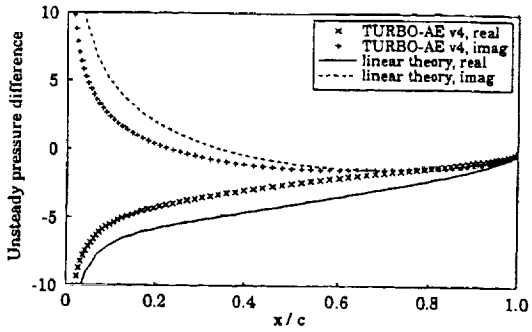

(g) 135 deg. pitching

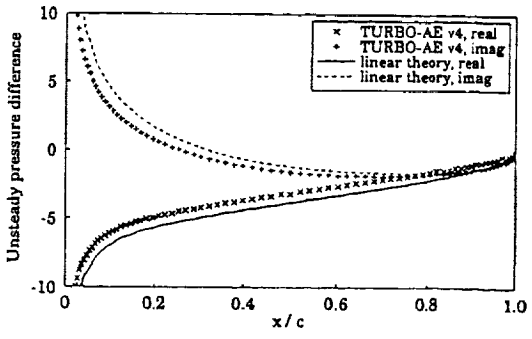

(h) 157.5 deg. pitching

Figure 5: Unsteady pressure difference (first harmonic) for pitching motion.

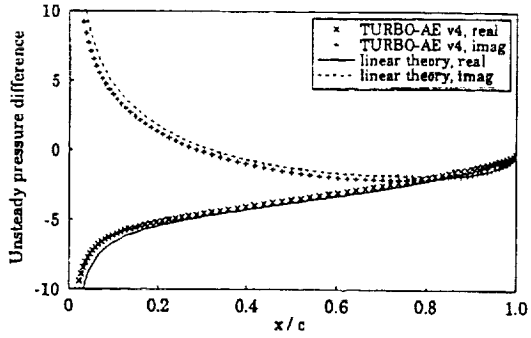

(i) 180 deg. pitching

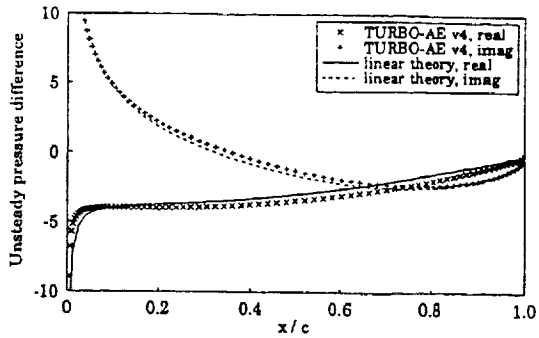

(m) 270 deg. pitching

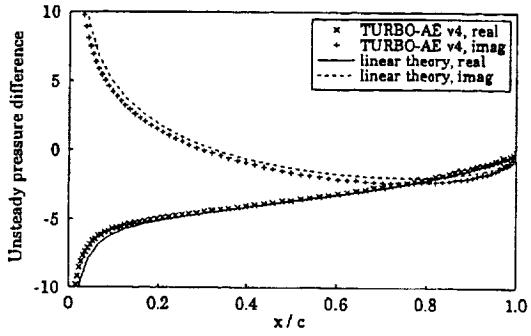

(j) 202.5 deg. pitching

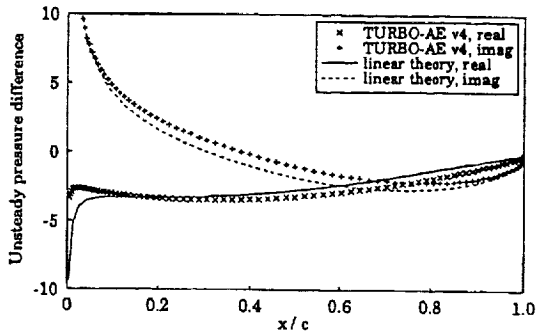

(n) 292.5 deg. pitching

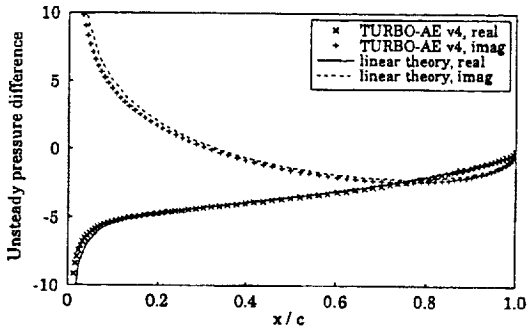

(k) 225 deg. pitching

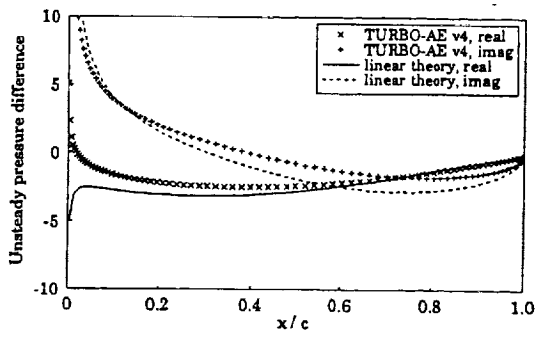

(o) 315 deg. pitching

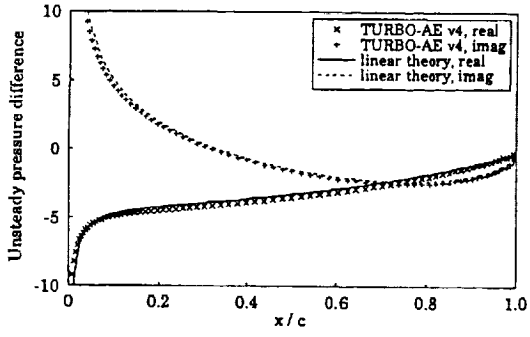

(l) 247.5 deg. pitching

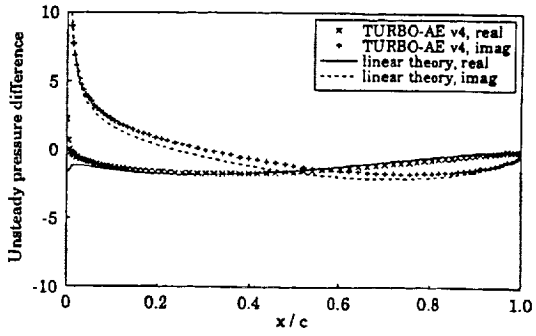

(p) 337.5 deg. pitching

Figure 5 (continued): Unsteady pressure difference (first harmonic) for pitching motion.

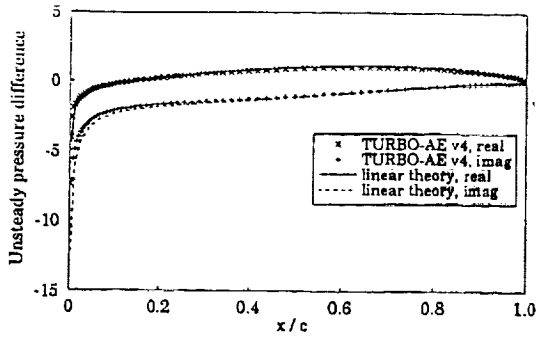

(a) 0 deg. plunging

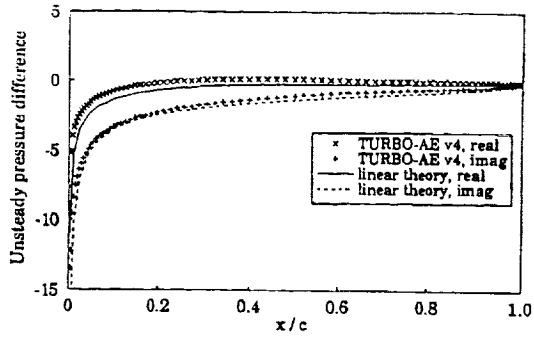

(e) 90 deg. plunging

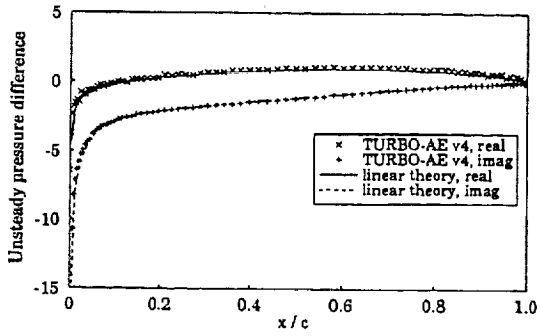

(b) 22.5 deg. plunging

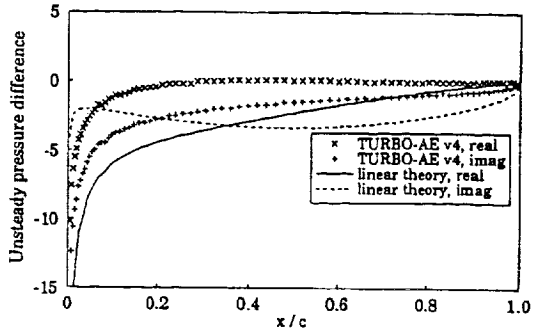

(f) 112.5 deg. plunging

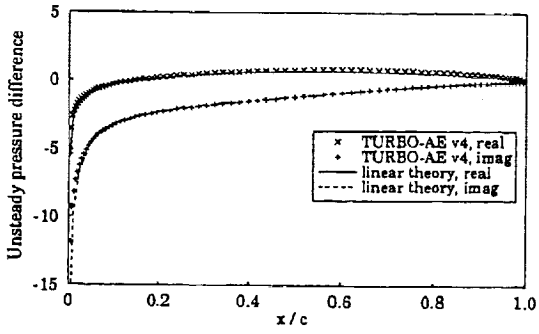

(c) 45 deg. plunging

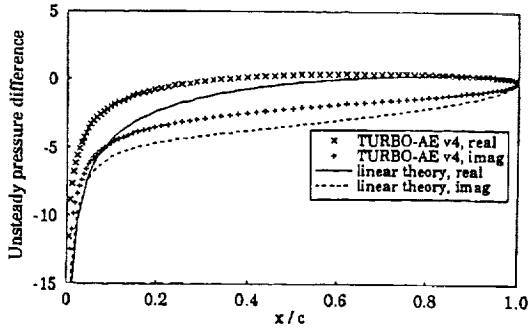

(g) 135 deg. plunging

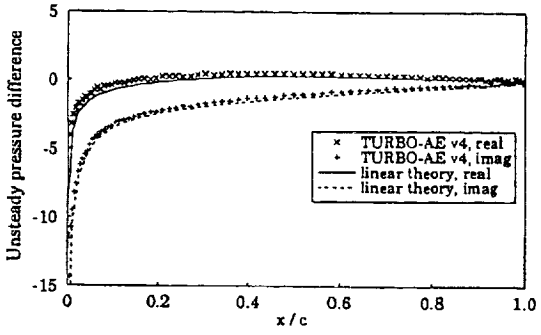

(d) 67.5 deg. plunging

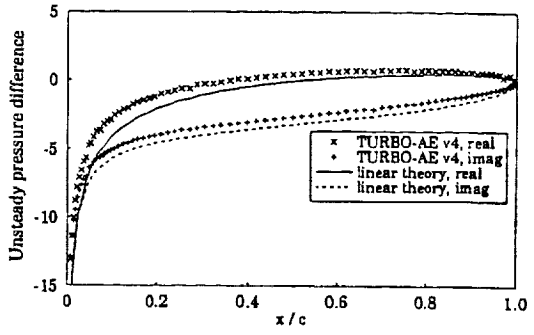

(h) 157.5 deg. plunging

Figure 6: Unsteady pressure difference (first harmonic) for plunging motion.

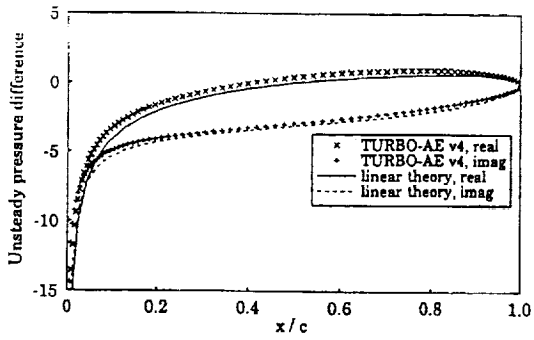

(i) 180 deg. plunging

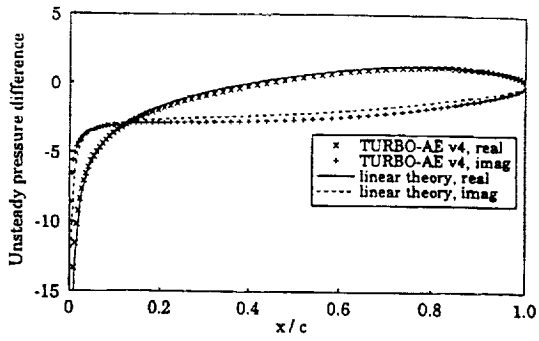

(m) 270 deg. plunging

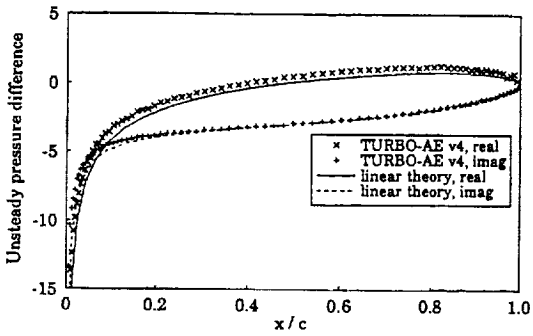

(j) 202.5 deg. plunging

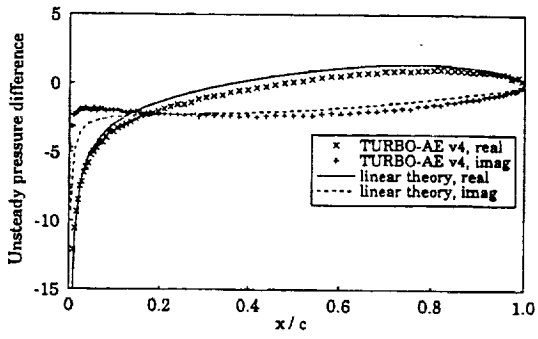

(n) 292.5 deg. plunging

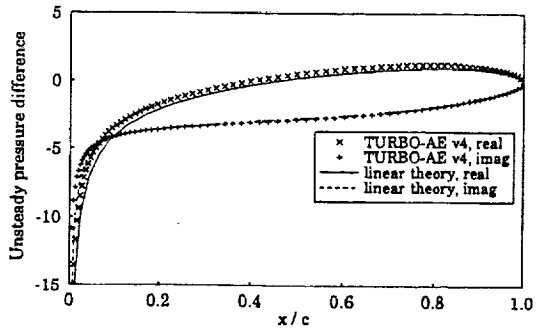

(k) 225 deg. plunging

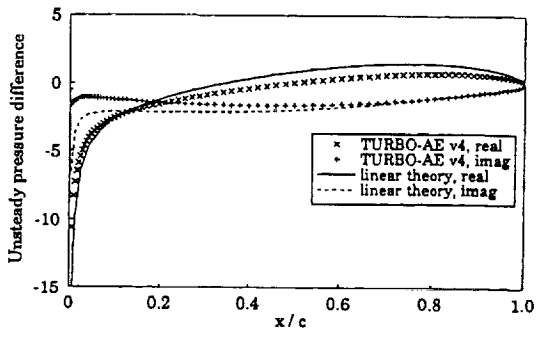

(o) 315 deg. plunging

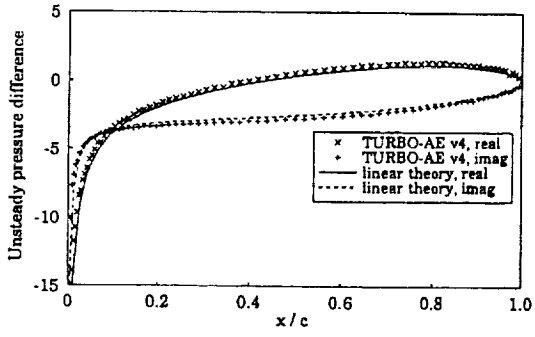

(l) 247.5 deg. plunging

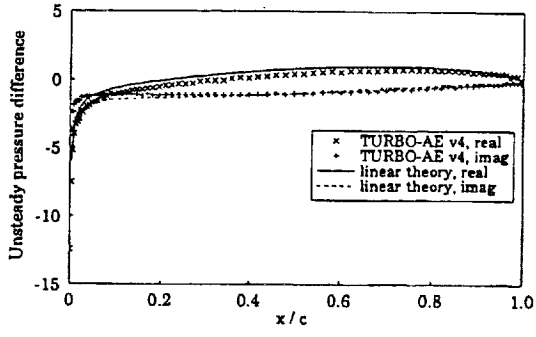

(p) 337.5 deg. plunging

Figure 6 (continued): Unsteady pressure difference (first harmonic) for plunging motion.